Modeling for multi-resonant behavior of broadband metamaterial absorber with geometrical substrate*

Kai-Lun Zhang(张凯伦)[1], Zhi-Ling Hou(侯志灵)[1,†], Song Bi(毕松)[2], and Hui-Min Fang(房惠敏)[1]

[1] School of Science & Beijing Key Laboratory of Environmentally Harmful Chemicals Assessment, Beijing University of Chemical Technology, Beijing 100029, China

[2] 501 Department, Xi'an Research Institute of High Technology, Xi'an 710025, China

(Received 31 July 2017; revised manuscript received 18 September 2017; published online 20 October 2017)

Despite widespread use for extending absorption bandwidth, the coexistence and coupling mechanism of multiple resonance is not well understood. We propose two models to describe the multi-resonant behavior of a broadband metamaterial absorber with geometrical-array substrate (GAS). The multi-resonance coupling of GAS is well described by logarithmic law. The interaction between metasurface and GAS can further broaden the absorption bandwidth by generating a new resonance which coexists with original resonances in substrate. The proposed models can thoroughly describe this multiple-resonance behavior, highlighting guidelines for designing broadband absorbers.

Keywords: metasurface, broadband absorption, dielectrics

PACS: 78.67.Pt, 77.22.–d, 52.25.Os **DOI:** 10.1088/1674-1056/26/12/127802

1. Introduction

Dielectric and magnetic materials of electromagnetic response capability have drawn significant attention in the aerospace industry due to the great applications in stealth technology[1–5] and energy usage.[6–9] In the GHz frequency range, traditional homogeneous absorbers[10–12] mainly rely on the establishment of resonance absorption, which is easy to achieve high absorption at sub-wavelength thickness. However, the absorption is efficient only in a narrow frequency band due to the thickness dependent resonance. With the progresses made in multiband or broadband communication technology, broadband absorption is highly desired. Many wideband absorbers with special structures are reported, including porous,[13] multilayer,[14] and pyramidal structures.[15] Unfortunately, these wideband absorbers were achieved at the sacrifice of the thickness. At a given thickness, metamaterial absorbers enable offering absorption peaks in either a lower or a higher frequency range to extend the absorption band. For instance, Wang *et al.*[16] fabricated a metamaterial absorber with a thickness of 1.60 mm and an over 90% absorption from 8.85 GHz to 14.17 GHz. Sui *et al.*[17] proposed a topology design of a broadband frequency selective surface absorber whose thickness is 3.60 mm for an effective frequency band from 6.68 GHz to 26.08 GHz. He *et al.*[18] realized a tunable polarization-independent wideband absorber owning a thickness of 4.15 mm for both C and X bands. Consequently, the design of metamaterial absorbers is considered to be a possible strategy for obtaining broadband absorbing materials.[19–26] Nevertheless, the design of metamaterial absorbers mainly focuses on periodically patterned resonators with the spacers usually constructed by a uniform dielectric sheet or air,[27–31] resulting in a thick multilayer structure corresponding to multiple resonance, which is necessary for achieving the broadband absorbers.[32,33] It is critical to increase resonance numbers for extending the absorption band at a limited thickness.[34–37] In fact, the geometrical design of traditional absorption material is also able to extend the absorption band at a limited thickness.[38,39] Therefore, a combination of single-layer metasurface with geometrical-array substrate (GAS) would efficiently increase the absorption band within a small thickness.

To understand the coexistence and coupling mechanism of multiple resonances in a broadband metamaterial absorber with the geometrical-array substrate, in this work, we propose the logarithmic law and equivalent circuit model to explain the multi-resonance coupling and coexistence in the broadband metamaterial absorber with the geometrical-array substrate. The consistence between the theoretical and simulated results suggests good comprehension of the strategy for designing broadband microwave absorption metamaterials.

2. Method

The simulations are all carried out in the microwave simulation software CST studio suite 2014. As shown in Fig. 1(a), TEM wave along the z axis is normally incident on GAS. Ideal electric field and magnetic field boundaries are used in calculation, all the diffraction beams are reflected, and only the intrinsic absorption of GAS is taken into the calculation of reflection

*Project supported by the National Natural Science Foundation of China (Grant No. 51302312), the Fund for Discipline Construction of Beijing University of Chemical Technology (Grant No. XK1702), and the Fundamental Research Funds for the Central Universities, China (Grant No. Jd1601)..

†Corresponding author. E-mail: zhilinghou@gmail.com

© 2017 Chinese Physical Society and IOP Publishing Ltd

loss. The GAS consists of two layers, where the top layer is a periodic square array with the period $a = 19$ mm and side length $w = 13.4$ mm, and the bottom layer is homogeneous. The thickness values of the square array and bottom layer are both 3 mm. The material of GAS has permittivity complying with a single Debye dielectric relaxation law (Fig. 1(b)), where static permittivity $\varepsilon_{r0} = 6.78$, optical permittivity $\varepsilon_{r\infty} = 1.93$, and relaxation time $\tau = 2.99 \times 10^{-11}$.

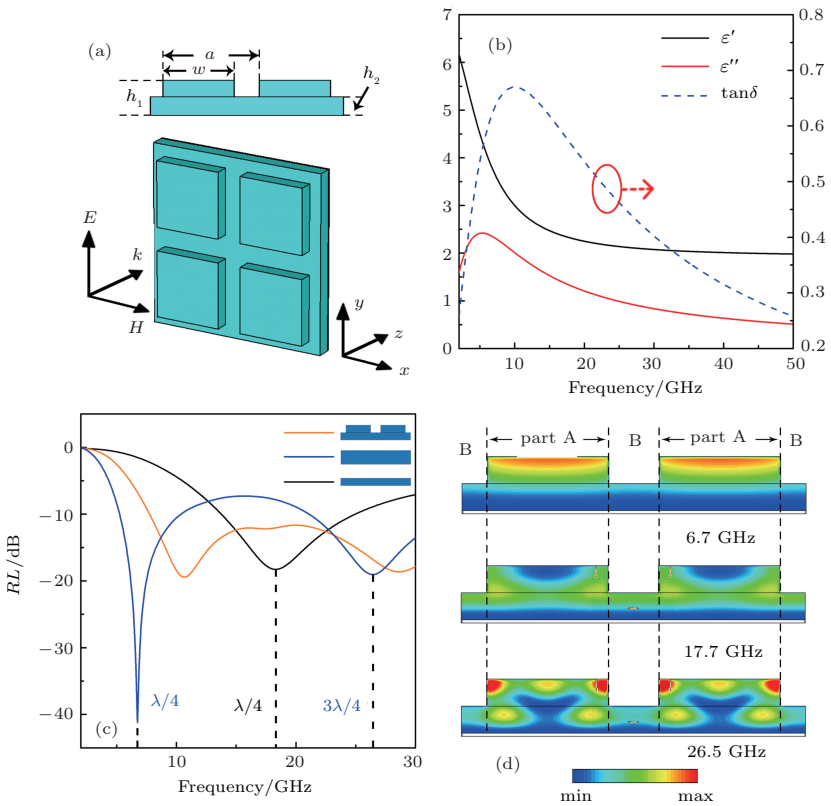


Fig. 1. (color online) (a) Three-dimensional view and structure size of the GAS, (b) permittivity and dielectric loss of the material, (c) reflection loss of GAS (orange line), 3 mm (black line) and 6 mm (blue line) plate, and (d) power loss of the GAS at 6.7 GHz (top), 17.7 GHz (middle), and 26.5 GHz (bottom).

3. Results and discussion

The absorption band (< -10 dB) of the GAS covers 7.76 GHz–30 GHz, which is much wider than those of the 3-mm and 6-mm plates (Fig. 1(c)). The widened absorption band is mainly contributed by the multiple resonances at different thickness values, including $\lambda/4$ resonance at 3 mm, $\lambda/4$ and $3\lambda/4$ resonances at 6 mm. The properly coupled essential $(2n+1)\,\lambda/4$ resonances in different thickness values can efficiently extend the absorption band. The coexistence of multiple resonances is confirmed by distributions of power loss of the GAS at different frequencies (Fig. 1(d)). The loss distributions along the z axis (top and middle of Fig. 1(d)) indicate the $\lambda/4$ resonances at 6.7 GHz in part A and at 17.7 GHz in part B. The bottom of Fig. 1(d) shows that the double-layer distributed power loss at 26.5 GHz is caused by $3\lambda/4$ resonance from part A. Nevertheless, the large loss intensity is observed at the top corner, suggesting that the edge scattering at higher frequency also affects the microwave absorption. The result of loss distribution shows that when the structure size is less than the microwave wavelength, the microwave absorption is mainly associated with the multiple $(2n+1)\,\lambda/4$ resonances of two thickness values.

Extending the absorption band by multiple $\lambda/4$ resonances in a patterned microwave absorber is confirmed experimentally.[38,39] The GAS can be equivalent to a composite material comprised of parts A and B (Fig. 1(d)). Considering that the defect size is much smaller than EM wavelength, part B is treated as a homogeneous effective dielectric with the same thickness as part A. So the total electromagnetic response can be characterized through the combination of part A and the effective part B. When part A is combined in parallel with part B (left of Fig. 2(a)), there is a linear relationship between the surface densities of polarization charges in different parts ($\sigma S = \sigma_1 S_1 + \sigma_2 S_2$). As $\sigma = \varepsilon_0 (\varepsilon_r - 1) E$, the effective permittivity of the composite material can be described as $\varepsilon_{\text{eff}} = x_1 \varepsilon_1 + x_2 \varepsilon_2$, where x_1 and x_2 are the area ratios of parts A and B, i.e., $x_1 = S_A/(S_A + S_B)$ and $x_2 = S_B/(S_A + S_B)$, with S_A and S_B being the areas of parts A and B, and ε_1 and ε_2 are the permittivities of parts A and B, respectively. Similarly, when part A is combined in series with part B (middle of Fig. 2(a)), the permittivity relationship can be expressed as $1/\varepsilon_{\text{eff}} = x_1/\varepsilon_1 + x_2/\varepsilon_2$. Thus, the permittivity of com-

posite dielectric material can be concluded as Lichtenecker's equation:[40,41]

$$\varepsilon_{\text{eff}}^{m} = \varepsilon_1^{m} x_1 + \varepsilon_2^{m} x_2, \tag{1}$$

where the power m varies within the $[-1,1]$ range. $m=1$ and $m=-1$ for the parallel and series combination of parts A and B, respectively. When the two kinds of combinations coexist in the proposed patterned absorber (right of Fig. 2(a)), m should be close to 0 and the differential form of Eq. (1) is

$$m\varepsilon_{\text{eff}}^{m-1}\,\mathrm{d}\varepsilon_{\text{eff}} = mx_1\varepsilon_1^{m-1}\,\mathrm{d}\varepsilon_1 + mx_2\varepsilon_2^{m-1}\,\mathrm{d}\varepsilon_2. \tag{2}$$

Due to $m=0$,

$$\frac{\mathrm{d}\varepsilon_{\text{eff}}}{\varepsilon_{\text{eff}}} = x_1\frac{\mathrm{d}\varepsilon_1}{\varepsilon_1} + x_2\frac{\mathrm{d}\varepsilon_2}{\varepsilon_2}, \tag{3}$$

and

$$\ln(\varepsilon_{\text{eff}}) = x_1\ln(\varepsilon_1) + x_2\ln(\varepsilon_2). \tag{4}$$

So, the permittivity of GAS can be expressed as[42]

$$\log\varepsilon_{\text{eff}} = x\log\varepsilon_1 + (1-x)\log\varepsilon_2, \tag{5}$$

where x is the area ratio of part A, i.e., $x=x_1$. The relationship between refractive index$n$ and resonance frequency f is

$$n = \frac{v_0}{4hf}, \tag{6}$$

where v_0 is the velocity of light. Because ε approximately equals n^2 for nonmagnetic material, and the effective permittivity of part B equals $\varepsilon_2 = [v_0/(16hf_2)]^2$, the relationship between resonance frequencies can be expressed as

$$\log f = x\log f_1 + (1-x)\log f_2, \tag{7}$$

where $f_1 = 6.75$ GHz and $f_2 = 18.32$ GHz are the resonance frequencies at 6-mm and 3-mm thickness, respectively. Moreover, figure 2(c) shows the plots of the area ratio dependence of peak frequency in Fig. 2(b), and the simulated data (red empty box) are in good agreement with theoretical results (black line).

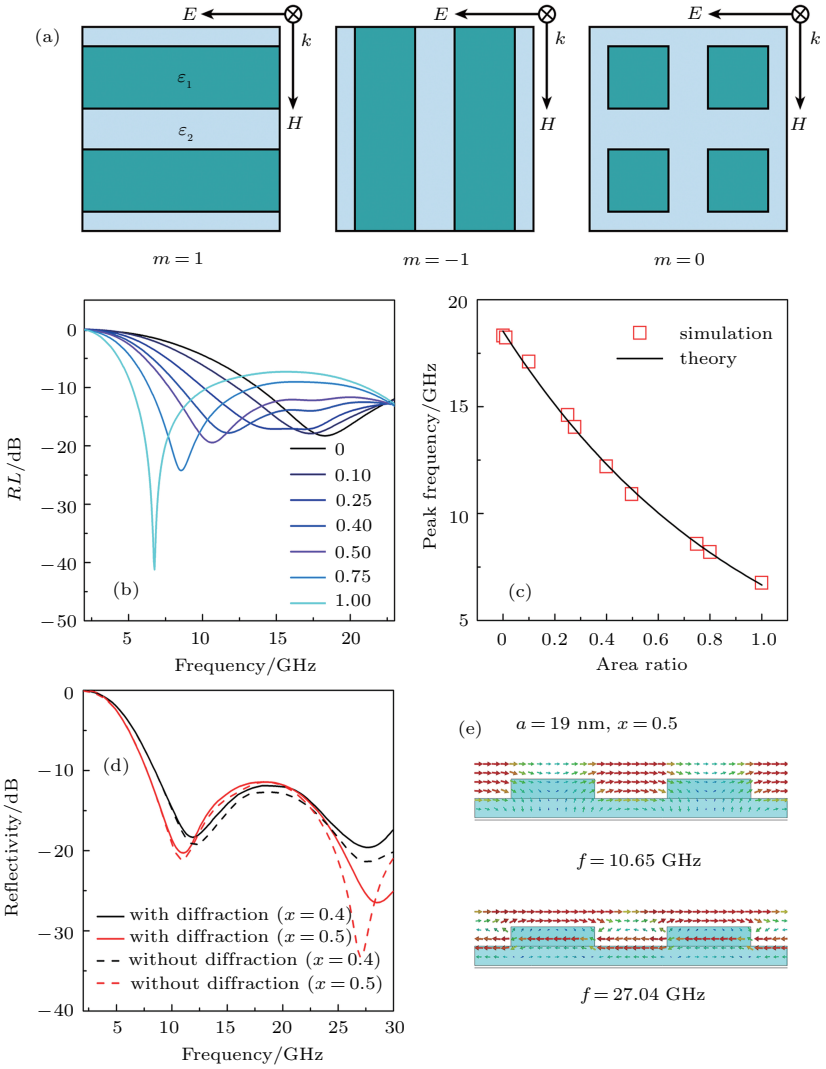


Fig. 2. (color online) (a) Schematic diagram of parallel (left), series (middle), and series-parallel combinations (right) of composites. (b) Frequency dependence of reflection loss of GAS with different area ratios, (c) area ratio dependence of peak frequency of the GAS; (d) comparison of calculated reflectivities with (including absorption) and without diffraction beam (including absorption and scattering), and (e) electric field distributions of 10.65 GHz and 27 GHz at area ratio $x=0.5$.

In order to clarify the influence of structure scattering, the typical Floquet port and unit cell boundary are used to calculate the reflectivity without diffraction beam. With structure size and material parameters fixed, the calculated reflectivities with (including absorption) and without diffraction beam (including absorption and scattering) are compared in Fig. 2(d). At two different area ratios, the structure scattering has a little influence on the lowest coupled resonance peak, implying the validity of Eq. (7) for the lowest resonance frequency calculation. With the enhancement of structure scattering at higher frequency, which can be confirmed by electric field distribution (Fig. 2(e)), the influence of structure scattering on the reflection peak becomes obvious. So, equation (7) is not applicable for calculating other absorbing peaks at higher frequency.

To enhance the absorption of the GAS at low frequency, a square copper ring is assembled on the top of each geometrical array. The thickness of the metasurface is as thin as 0.1 mm. The side length l and width d of each of copper ring are set to be $l = 8$ mm and $d = 0.5$ mm, respectively. The minimum frequency of reflection loss $\leqslant -10$ dB for the GAS is 7.76 GHz (Fig. 3(a)), and it is extended to 4.75 GHz due to the introduction of the metasurface (Fig. 3(b)). Apparently, the essential absorption peak (β peak) frequency of GAS is 10.65 GHz. The new absorption peak (α peak) induced by interaction between metasurface and GAS appears at 5.45 GHz (Fig. 3(b)).

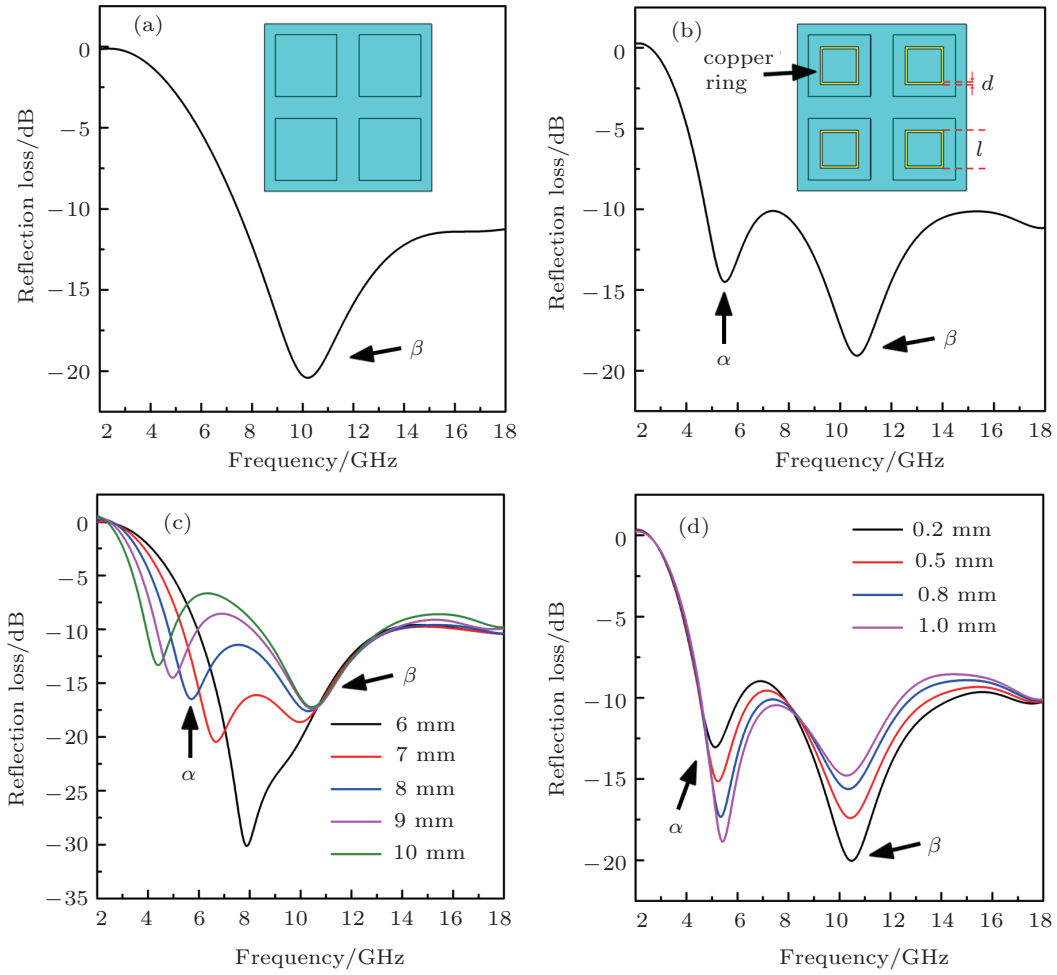


Fig. 3. (color online) (a) Reflection loss of GAS, (b) reflection loss of metamaterial absorber with GAS at $l = 8$ mm and $d = 0.5$ mm, (c) reflection losses at different side lengths, and (d) reflection losses at different widths for metamaterial absorber with GAS.

The α peak is dominated by side length l and width d. As shown in Fig. 3(c), the frequency of the α peak is mainly dependent on the side length l, while the frequency of the β peak remains unchanged. As l increases from 6 mm to 10 mm, the α resonance frequency decreases. The peak frequency of the α peak shifts from 7.89 GHz to 4.4 GHz. However, the frequencies of the α and β peaks are almost independent of the width d (see Fig. 3(d)). On the other hand, the width d has influences on the absorption intensity of both α and β peaks. When d increases from 0.2 mm to 1 mm, the intensity of the β peak is weakened while the α peak is enhanced. The diminishing of the β peak with increasing d results from the impedence mismatch between metasurface and air at high frequency, so d should be optimized to both enhance low-frequency absorption and keep the high-frequency absorption. Therefore, the frequency and intensity of the α peak can be adjusted by changing l and d, respectively.

Figures 4(a) and 4(b) show the power loss and the surface

current of the metamaterial absorber with GAS at 5.45 GHz. The energy loss is mainly distributed nearby the metal ring arrays of the metamaterial absorber with GAS (see Fig. 4(a)), which supports that the absorption peaks appear at lower frequencies in Fig. 3(d). On the basis of the surface current distribution (see Fig. 4(b)), an equivalent *RLC* series resonance circuit model[43] is used to describe the interaction between the metasurface and GAS. The resonance frequency is known to have the following form

$$f = \frac{1}{2\pi\sqrt{LC}}, \tag{8}$$

where, the equivalent inductance L can be expressed as follows:

$$L = \frac{m\mu_0 l^2 N^2}{4l}, \tag{9}$$

and the equivalent capacitance C can be written as the following form

$$C = \frac{4\varepsilon_0\varepsilon_r ld + n}{4h_1}, \tag{10}$$

where $h_1 = 6$ mm is the thickness of dielectric material, l and d are the side length and width of square copper ring, respectively, $N = 1$ the number of rings in the propagation direction of the microwave, $n = 0.78$ and $m = 1.53$ are the correction factors for the fringe capacitance and the shape coefficient of the inductance of square ring, respectively; $\varepsilon_0 = 8.85 \times 10^{-12}$ and $\mu_0 = 1.26 \times 10^{-6}$ are the vacuum permittivity and permeability, respectively. The relative permittivity ε_r of GAS material is given by Debye equation

$$\varepsilon_r = \varepsilon_{r\infty} + (\varepsilon_{r0} - \varepsilon_{r\infty})\frac{1}{1+\omega^2\tau^2}. \tag{11}$$

By combining Eqs. (8), (9), (10), and (11), the relation can be written as

$$\frac{1}{f} = \sqrt{F_1(F_2 + F_3 l^2) + \sqrt{F_4 l^2 + F_5(F_2 + F_3 l^2)^2}}. \tag{12}$$

Here, the coefficients are $F_1 = -83.33$, $F_2 = 2.11 \times 10^{-22}$, $F_3 = -3.76 \times 10^{-18}$, $F_4 = 1.25 \times 10^{-35}$, and $F_5 = 6.94 \times 10^3$, which are theoretically calculated from the simultaneous equations.

According to the Taylor formula, equation (12) can be simplified into the following form

$$\frac{1}{f} = -2.87 \times 10^{-11} l + 2.55 \times 10^{-8}. \tag{13}$$

Figure 4(c) shows the dependence of the side length of the copper ring on the resonance frequency induced by the periodic ring array. The prediction results of Eq. (12) are in good agreement with simulation data. Moreover, the relationship between side length and reciprocal of frequency can be well described by the linear Eq. (13) in the investigated frequency range (Fig. 4(d)). Therefore, the equivalent circuit model is valid for describing the dependence of this resonance on the surface metallic cell size.

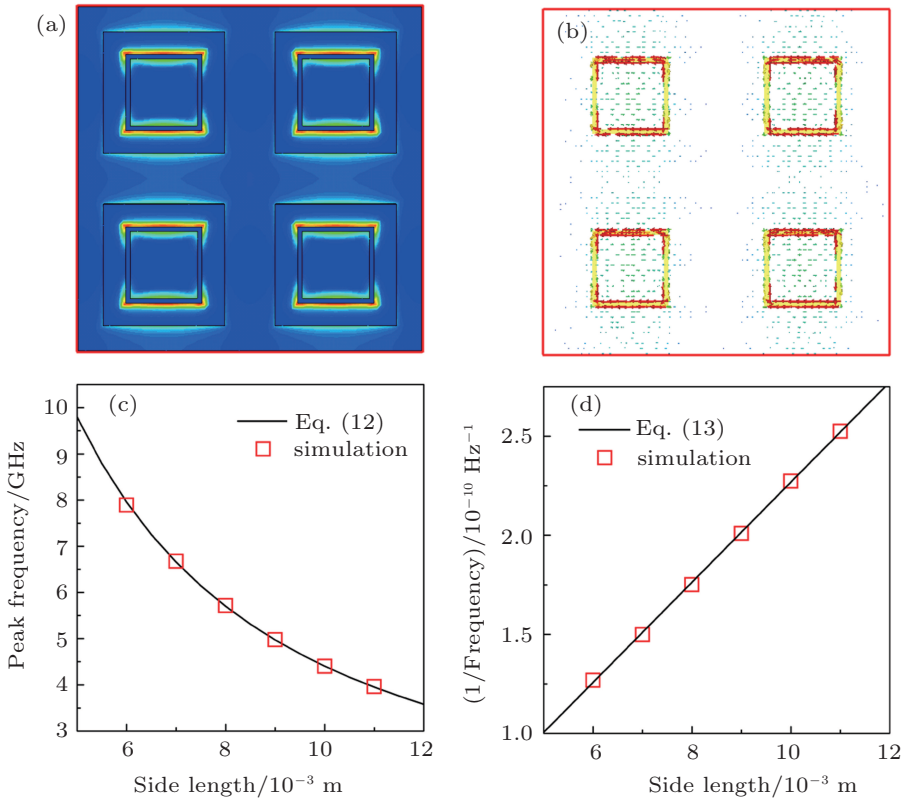


Fig. 4. (color online) (a) Power loss and (b) surface current of metamaterial absorber with GAS at 5.45 GHz, (c) peak frequency versus side length, and (d) reciprocal of peak frequency versus side length.

4. Conclusions

In this work, a broadband metamaterial absorber with geometrical substrate is proposed. The GAS broadens the absorption band by coupling multiple $\lambda/4$ resonances, and the area ratio dependence of resonance frequency for GAS is well described by logarithmic law. The interaction between metasurface and GAS generates a new resonance coexisting with original resonances in the substrate, resulting in the further increase of absorption bandwidth. According to the equivalent resonance circuit, we develop a quantitative model that completely describes the dependence of this resonance on the surface metallic cell size. This work, therefore, is helpful for understanding and utilizing multiple resonances in broadband absorption metamaterials.

References

[1] Liu Q H, Cao Q, Bi H, Liang C Y, Yuan K P, She W, Yang Y J and Che R C 2016 *Adv. Mater.* **28** 486

[2] Zhu H, F Yi and Cubukcu E 2016 *Nat. Photon.* **10** 709

[3] Fu C, He D W, Wang Y S, Fu M, Geng X and Zhuo Z L 2015 *Chin. Phys. B* **24** 087801

[4] Huang H L, H. Xia, Guo Z B, Chen Y and Li H J 2017 *Chin. Phys. B* **26** 025207

[5] Liang J J, Huang Y, Zhang F, Li N, Ma Y F, Li F F and Chen Y S 2014 *Chin. Phys. B* **23** 088802

[6] Bao Y H, Zhang X Y, Zhang X, Yang L, Zhang X Y, Chen H S, Yang M and Fang D N 2016 *J. Power Sources* **321** 120

[7] Zhang X Y, Chen H S and Fang D N 2016 *J. Solid State Electrochem.* **20** 2835

[8] Wei K, Chen H S, Pei Y M and Fang D N 2016 *J. Mech. Phys. Solids* **86** 173

[9] Zhang X Y, Yang L, Hao F, Chen H S, Yang M and Fang D N 2015 *Nanomaterials* **5** 1985

[10] Sudeep P M, Vinayasree S, Mohanan P, Ajayan P M, Narayanan T N and Anantharaman M R 2015 *Appl. Phys. Lett.* **106** 221603

[11] Chen Y J, Xiao G, Wang T S, Ouyang Q Y, Qi L H, Ma Y, Gao P, Zhu C L, Cao M S and Jin H B 2011 *J. Phys. Chem. C* **115** 13603

[12] Kong L, Yin X W, Yuan X Y, Zhang Y J, Liu X M, Cheng L F and Zhang L T 2014 *Carbon* **73** 185

[13] Zhang Y, Huang Y, Zhang T F, Chang H C, Xiao P S, Chen H H, Huang Z Y and Chen Y S 2015 *Adv. Mater.* **27** 2049

[14] Danlee Y, Huynen I and Bailly C 2012 *Appl. Phys. Lett.* **100** 213105

[15] Ding F, Cui Y X, Ge X C, Jin Y and He S L 2012 *Appl. Phys. Lett.* **100** 103506

[16] Wang B Y, Liu S B, Bian B R, Mao Z W, Liu X C, Ma B and Chen L 2014 *J. Appl. Phys.* **116** 094504

[17] Sui S, Ma H, Wang J F, Pang Y Q and Qu S B 2015 *J. Phys. D: Appl. Phys.* **48** 215101

[18] He Y, Jiang J J, Chen M, Li S C, Miao L and Bie S W 2016 *J. Appl. Phys.* **119** 105103

[19] Landy N I, Sajuyigbe S, Mock J J, Smith D R and Padilla W J 2008 *Phys. Rev. Lett.* **100** 207402

[20] Wen Q Y, Zhang H W, Yang Q H, Chen Z, Long Y, Jing Y L, Lin Y and Zhang P X 2012 *J. Phys. D: Appl. Phys.* **45** 235106

[21] Ye D X, Wang Z Y, Xu K W, Li H, Huangfu J T, Wang Z and Ran L X 2013 *Phys. Rev. Lett.* **111** 187402

[22] Xu B Z, Guo C Q, Li Z, Liu L L and Niu Z Y 2014 *J. Phys. D: Appl. Phys.* **47** 255103

[23] He X J, Yan S T, Ma Q X, Zhang Q F, Jia P, Wu F M and Jiang J X 2015 *Opt. Commun.* **340** 44

[24] Shen Y, Pang Y Q, Wang J F, Ma H, Pei Z B and Qu S B 2015 *J. Phys. D: Appl. Phys.* **48** 445008

[25] Chen K, Jia N, Sima B Y, Zhu B, Zhao J M, Feng Y J and Jiang T 2015 *J. Phys. D: Appl. Phys.* **48** 455304

[26] Liu L G and Cha H 2014 *J. Phys. D: Appl. Phys.* **47** 075105

[27] Shen X P, Cui T J, Zhao J M, Ma H F, Jiang W X and Li H 2011 *Opt. Express* **19** 9401

[28] Wang H, Kong P, Cheng W T, Bao W Z, Yu X W, Miao L and Jiang J J 2016 *Sci. Rep.* **6** 23081

[29] Wan M L, He J N, Song Y L and Zhou F Q 2015 *Phys. Lett. A* **379** 1791

[30] Xu W H, He Y, Kong P, Li J L, Xu H B, Miao L, Bie S W and Jiang J J 2015 *J. Appl. Phys.* **118** 184903

[31] Li H, Yuan L H, Zhou B, Shen X P, Cheng Q and Cui T J 2011 *J. Appl. Phys.* **110** 014909

[32] Zadeh A K and Karlsson A 2009 *IEEE T. Antenn. Propag.* **57** 2307

[33] Li M, Xiao S Q, Bai Y Y and Wang B Z 2012 *IEEE Antenn. Wirel. Pr.* **11** 748

[34] Li Z J, Hou Z L, Song W L, Liu X D, Cao Q X, Shao X H and Cao M S 2016 *Nanoscale* **8** 10415

[35] Jing L Q, Wang Z J, Yang Y H, Zheng B, Liu Y M and Chen H S 2017 *Appl. Phys. Lett.* **110** 231103

[36] Liu X M, Lan C W, Bi K, Li B, Zhao Q and Zhou J 2016 *Appl. Phys. Lett.* **109** 062902

[37] Zhang C, Cheng Q, Yang J, Zhao J and Cui T J 2017 *Appl. Phys. Lett.* **110** 143511

[38] Song W L, Zhang K L, Chen M J, Hou Z L, Chen H S, Yuan X J, Ma Y B and Fang D N 2017 *Carbon* **118** 86

[39] Zhou Q, Yin X W, Ye F, Liu X F, Cheng L F and Zhang L T 2017 *Mater. Design* **123** 46

[40] Lichtenecker K 1926 *Phys. Z.* **27** 115

[41] Goncharenko A V, Lozovski V Z and Venger E F 2000 *Opt. Commun.* **174** 19

[42] Fan B H, Zha J W, Wang D R, Zhao J and Dang Z M 2012 *Appl. Phys. Lett.* **100** 092903

[43] Haghzadeh M and Akyurtlu A 2016 *J. Appl. Phys.* **120** 184901